ELECTRONIC SUPPLEMENTARY INFORMATION

Anodization of large area Ti: versatile material for caffeine photodegradation and hydrogen production

Marcel Sihor,[a,b,#] Muhammad Bilal Hanif, [a,#] Guru Karthikeyan Thirunavukkarasu,[a] Viktoriia Liapun,[a] Miroslava Filip Edelmannova,[b] Tomas Roch,[c] Leonid Satrapinskyy,[c] Tomas Plecenik,[c] Sajid Rauf,[d] Karol Hensel,[e] Olivier Monfort,[a] and Martin Motola[a,*]

[a]Department of Inorganic Chemistry, Faculty of Natural Sciences, Comenius University in Bratislava, Ilkovicova 6, 842 15 Bratislava, Slovakia.

[b]Institute of Environmental Technology, CEET, VSB-Technical University of Ostrava, 17. listopadu 15/2172, Ostrava-Poruba, 708 00Czech Republic.

[c] Department of Experimental Physics, Faculty of Mathematics, Physics, and Informatics, Comenius University in Bratislava, 842 48 Bratislava, Slovakia.

[d]College of Electronics and Information Engineering, Shenzhen University, Guangdong Province, 518000, China

[e]Division of Environmental Physics, Faculty of Mathematics, Physics, and Informatics, Comenius University in Bratislava, 842 48 Bratislava, Slovakia.

*Corresponding author: Martin Motola martin.motola@uniba.sk

# Equal contribution

Text S1. Photoelectrochemical Measurements

Photoelectrochemical measurements were performed using a photoelectric spectrometer with a 150W Xe lamp used as an irradiation source equipped with a P-IF 1.6 potentiostat (Instytut Fotonowy, Poland). A three-electrode photoelectrochemical cell consisting of TNSs samples (working electrode), saturated Ag/AgCl electrode (reference electrode), and Pt electrode (counter electrode), respectively were immersed in 0.2 M KNO_3 electrolyte solution. The photocurrent transients were recorded under 300 to 420 nm wavelength light irradiation.

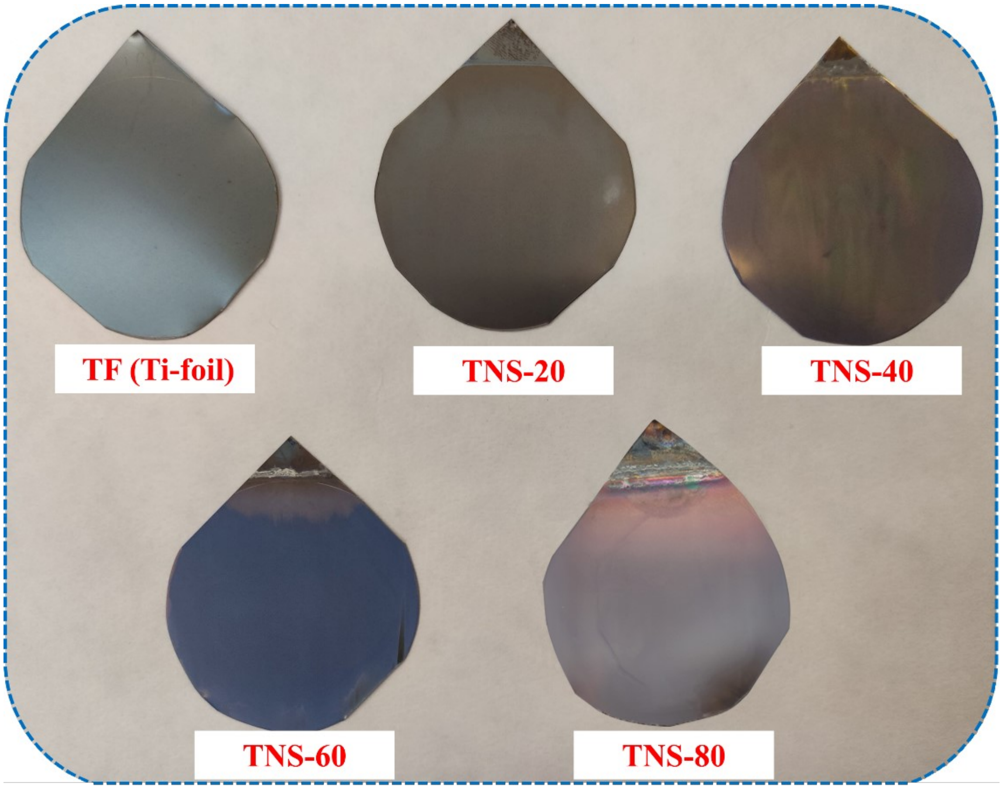

Fig. S1 Titanium foil (of different voltages) after the anodization and calcination process.

Fig. S2 Schematic representation of home-made photocatalytic reactor.

Fig. S3 The batch photoreactor used in the photocatalytic decomposition of methanol.

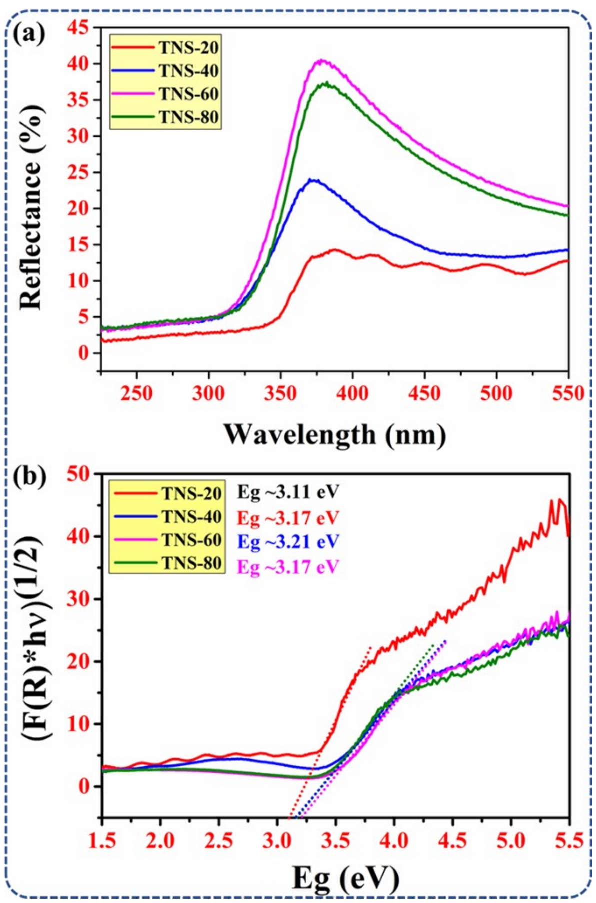

Fig. S4 (a) UV-VIS DRS and (b) Tauc plot with the E_g of TNS-20, TNS-40, TNS-60, and TNS-80, respectively.

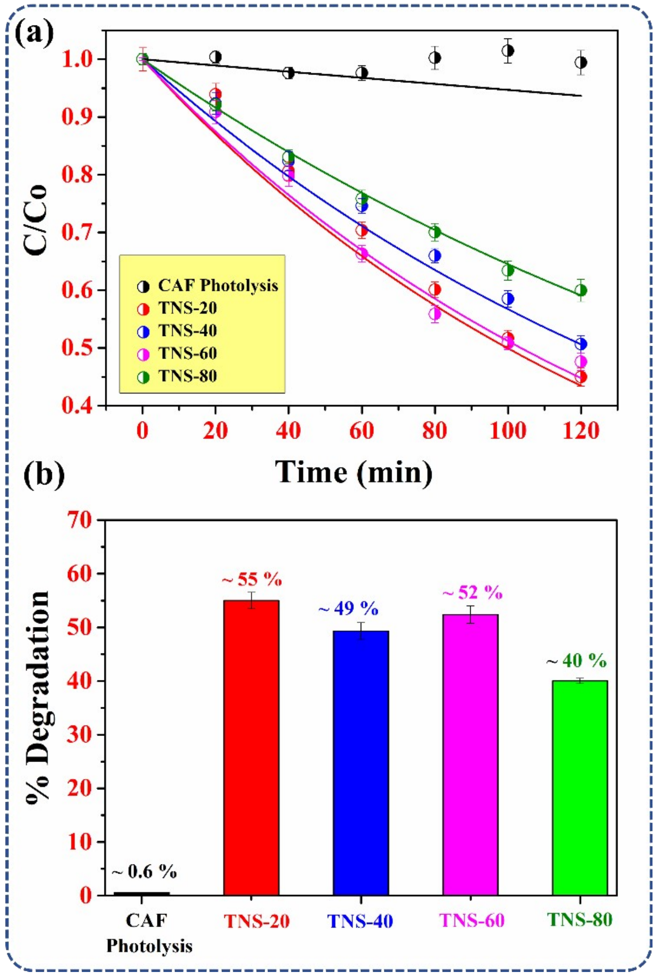

Fig. S5 Photocatalytic degradation of caffeine using TNSs samples (a) C/C_0 curves and (b) degradation % under UV-A irradiation.

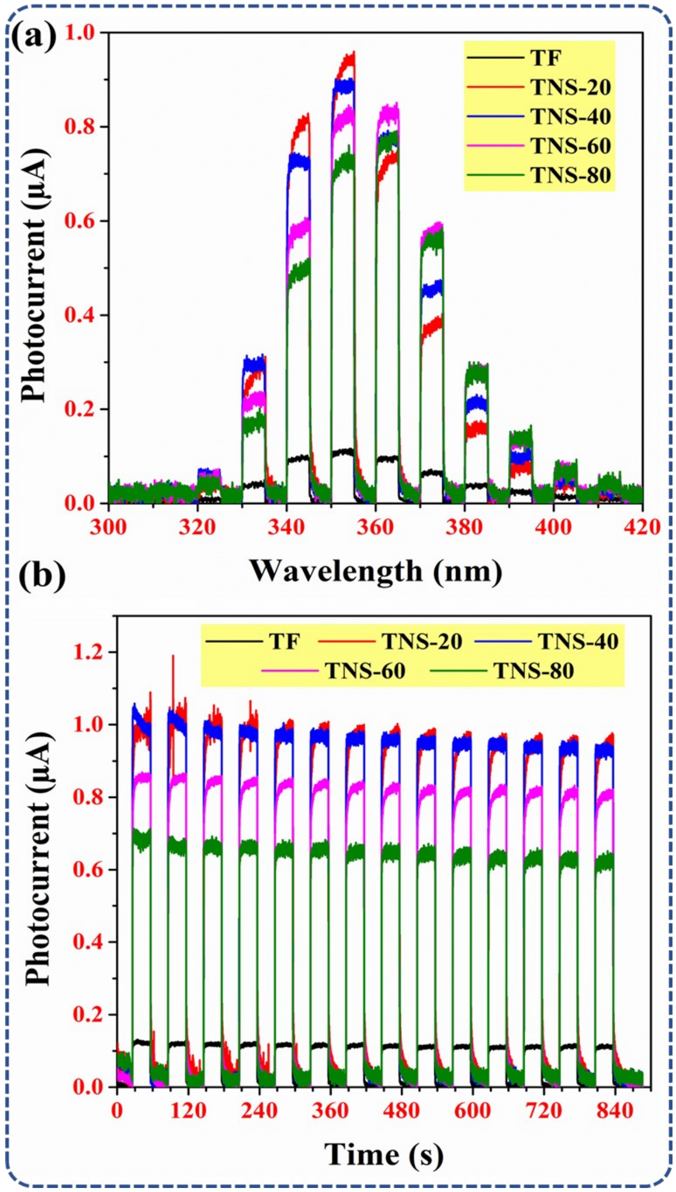

Fig. S6 (a) Photocurrent densities of TNSs samples with (b) corresponding transient currents from 300 to 420 nm.

Table S1: The electrochemical anodization parameters during the synthesis of TNS samples.

Sample	Voltage (V)	Time (min)	Current Density (A) Starting	Current Density (A) Ending
TF	-	-	-	-
TNS-20	20	100	0.305	0.040

TNS-40	40	100	0.370	0.035
TNS-60	60	100	0.320	0.035
TNS-80	80	100	0.361	0.039

Table S2: The Average Roughness (S_a), Root Mean Square (S_q), and Surface Skewness (S_{sk}), and Coefficient of Kurtosis (S_{ka}) values obtained from atomic force microscopy.

Sample	Average Roughness S_a (nm)	Root Mean Square S_q (nm)	Surface Skewness S_{sk}	Coefficient of kurtosis S_{ka}
TF	43.625	55.858	0.110	0.191
TNS-20	74.039	92.373	0.423	-0.097
TNS-40	61.691	78.719	0.212	0.516
TNS-60	81.298	102.138	0.359	0.063
TNS-80	122.047	150.843	0.187	-0.352

Table. S3: A summary of different areas of TiO_2 photocatalysts under UV light irradiation. Wherever was possible, the area, parameters, target pollutant with its concentration, rate constants, time duration, and H_2 production were supplemented from the given references.

Material	Area	Anodization conditions	Target pollutant and concentration	Pollutant Degradation rate (*k*)/ Percentage (%)	Time *(min)*	H_2 production	Ref
TNT-10um	(10×50× 0.1 mm)	3-vol% H_2O + 0.5-wt% NH_4F in EG electrolyte (60V for 2-20 min)	Acid orange (25 µM)	0.019 min^{-1}	150	---	[1]
TiO_2-NTs	146.09 mm^2	95 : 5 wt% ethylene glycol/water containing 0.15M NH_4F (40 V for 20 min)	---	---	---	---	[2]
TNT- TiO_2	5×10 cm^2	176 mM NH_4F + 1.5 vol% DI-H_2O (60 V for 4 h)	---	---	---	---	[3]
TNTs+2c MoS_2	2.25 cm^2	Prepared by atomic layer deposition	Methylene blue ($1x10^{-5}$ M)	0.0190 min^{-1}	120	---	[4]
TiO_2	12.5 cm^2	0.3 wt.% NH_4F and 2 vol.% H_2O in -EG electrolyte	---	---	---	---	[5]

		(60 V for 72 h)					
TiO_2-SG	5×10 cm^2	0.5 wt% -EG electrolyte + NH_4F and 0.2 wt% DI-H_2O (40V for 4 h)	Methylene blue ($3x10^{-5}$ M)	0.003 s^{-1}	---	---	6
TiO_2	50 cm^2	0.3 wt.% of NH_4F +2 vol.% of DI-H_2O in an ethylene glycol electrolyte (60 V for 6 h)	Caffeine (50 mM.)	44%	180	---	7
Pine-cone TiO_2	30 mm × 40 mm	0.6 wt % NH_4F -10 vol % H_2O-EG electrolyte (60 V for 2 h)	Methylene orange (20.0 mM)	85%	120	---	8
TiO_2NTs@ Fe_3O_4	2.25 cm^2	0.15 M NH_4F + 10% DI-H_2O in glycol-based electrolyte (100 V for 4 h)	Methylene blue ($1×10^{-5}$ M)	0.38 h^{-1}	120	---	9
TiO_2	10 mm x 15 mm	0.5 wt.% NH_4F+10% DI-H_2O + 90 vol.% EG (30 V for 1 h)	Methylene orange	0.00040 min^{-1}	240	---	10
TiO_2 film	25 × 25 × 1 mm	NH_4F (0.3 wt %) and H_2O (2 vol%) in EG (60V for 3h)	Caffeine (10 $mg.L^{-1}$)	1.882 $mmol.L^{-1}.h^{-1}$	---	---	11
TiO_2 nanotube films	98.5 mm diamter	NH_4F (0.3 wt %) and H_2O (2 vol%) in EG (60V for 6 h)	Caffeine (50 $mg.L^{-1}$)	60%/ 0.014 x 10^{-6} $mol.L^{-1}$	180	---	12
TiO_2 NTs	---	NH_4F (0.3 wt %) and H_2O (2 vol%) in EG (60V for 3 h)	Caffeine 10 ppm	1.65 x 10^{-2} min^{-1}	180	---	13
V-TNT	~0.79 cm^2	1.3 g NH_4F + 197 mL EG + 3 mL H_2O (60 V for 4 h)	Caffeine (20 ppm)	3.25 x 10^{-3} min^{-1}	120	---	14
TNS-20	**~20 cm^2**	**2g NH_4F +100 ml DI-H_2O in glycerol-based electrolyte (20 V for 100 min)**	**Caffeine (20 ppm)**	**0.0069 min^{-1}**	**120**	**~6200 ppm**	**This Study**

References

1 H. Il Kim, D. Kim, W. Kim, Y. C. Ha, S. J. Sim, S. Kim and W. Choi, *Appl. Catal. A Gen.*, 2016, 174–181.

2 E. Mena, M. J. Martín de Vidales, S. Mesones and J. Marugán, *Catal. Today*, 2018, **313**, 33–39.

3 H. Sopha, M. Baudys, M. Krbal, R. Zazpe, J. Prikryl, J. Krysa and J. M. Macak, *Electrochem. commun.*, 2018, **97**, 91–95.

4 M. Motola, M. Baudys, R. Zazpe, M. Krbal, J. Michalička, J. Rodriguez-Pereira, D. Pavliňák, J. Přikryl, L. Hromádko, H. Sopha, J. Krýsa and J. M. Macak, *Nanoscale*, 2019, **11**, 23126–23131.

5 M. Paulose, L. Peng, K. C. Popat, O. K. Varghese, T. J. LaTempa, N. Bao, T. A. Desai and C. A. Grimes, *J. Memb. Sci.*, 2008, **319**, 199–205.

6 M. Motola, L. Satrapinskyy, T. Roch, J. Šubrt, J. Kupčík, M. Klementová, M. Jakubičková, F. Peterka and G. Plesch, *Catal. Today*, 2017, **287**, 59–64.

7 L. Suhadolnik, Ž. Marinko, M. Ponikvar-Svet, G. Tavčar, J. Kovač and M. Čeh, *J. Phys. Chem. C*, 2020, **124**, 4073–4080.

8 Y. Liu, Y. Zhang, L. Wang, G. Yang, F. Shen, S. Deng, X. Zhang, Y. He, Y. Hu and X. Chen, *Catal. 2017, Vol. 7, Page 229*, 2017, **7**, 229.

9 D. Beketova, M. Motola, H. Sopha, J. Michalicka, V. Cicmancova, F. Dvorak, L. Hromadko, B. Frumarova, M. Stoica and J. M. Macak, *ACS Appl. Nano Mater.*, 2020, **3**, 1553–1563.

10 H. Li, L. Cao, W. Liu, G. Su and B. Dong, *Ceram. Int.*, 2012, **38**, 5791–5797.

11 M. Krivec, K. Žagar, L. Suhadolnik, M. Čeh and G. Dražić, *ACS Appl. Mater. Interfaces*, 2013, **5**, 9088–9094.

12 L. Suhadolnik, Ž. Marinko, M. Ponikvar-Svet, G. Tavčar, J. Kovač and M. Čeh, *J. Phys. Chem. C*, 2020, **124**, 4073–4080.

13 Ž. Marinko, L. Suhadolnik, B. Šetina Batič, V. S. Šelih, B. Majaron, J. Kovač and M. Čeh, *ACS Omega*, 2021, **6**, 23233–23242.

14 G. K. Thirunavukkarasu, S. Gowrisankaran, M. Caplovicova, L. Satrapinskyy, M. Gregor, A. Lavrikova, J. Gregus, R. Halko, G. Plesch, M. Motola and O. Monfort, *Dalt. Trans.*, , DOI:10.1039/D2DT00829G.